ISSN (Print) 1226-1750
ISSN (Online) 2233-6656
Journal of Magnetics 26(3), 249-255 (2021) https://doi.org/10.4283/JMAG.2021.26.3.249

Parameterization of Multi Band Model of Critical Magnetic Fields for the Iron based Superconductor $Ba(Fe_{1-x}Ni_x)_2As_2$

Teklie Lissanu Tegegne[1]* and Gebregziabher Kahsay[2]

[1]*Department of Physics, College of Science, Assosa University, Assosa, Ethiopia*
[2]*Department of Physics, College of Science, Bahir Dar University, Bahir Dar, Ethiopia*

(Received 2 March 2021, Received in final form 5 July 2021, Accepted 7 July 2021)

In this study, the mathematical expression of temperature dependence upper critical magnetic field (H_{c2}), angle dependence of upper critical magnetic field (H_{c2}), and temperature dependence of Ginzburg-Landau (GL) characteristics were investigated. The parameters were computed by using two band Ginzburg-Landau (GL) phenomenological model for $Ba(Fe_{1-x}Ni_x)_2As_2$ iron based superconductor. Application of very small external magnetic field at low temperature to nickel doped $BaFe_2As_2$ changes to $Ba(Fe_{1-x}Ni_x)_2As_2$ iron based superconductor at a critical temperature of 19.5 K. The phase diagrams of the two upper-critical field and GL characteristics length were plotted as a function of angle and temperature for $Ba(Fe_{1-x}Ni_x)_2As_2$ iron based superconductor using the experimental values. The phase diagram shows the linear dependence of upper critical magnetic field parallel $H_{c2}^{\parallel c}$ and perpendicular ($H_{c2}^{\perp c}$) with temperature (T). Correspondingly, the phase diagrams of the upper critical field ($H_{c2}(\theta)$) versus the angle (θ) were plotted. The parallel and perpendicular to the symmetry axis of coherence length (ξ_{GL}(T)) and penetration depth ($\lambda_{GL}(T)$) versus temperature were plotted. In these plots both parameters are increased with increasing temperature and diverges at the critical temperature for the superconductor $Ba(Fe_{1-x}Ni_x)_2As_2$. This theoretical investigation was found to be in agreement with the obtained experimental results.

Keywords : two band $Ba(Fe_{1-x}Ni_x)_2As_2$, upper critical magnetic field ($H_{c2}(T)$), GL coherence length ($\xi_{GL}(T)$), GL penetration depth ($\lambda_{GL}(T)$)

1. Introduction

The great discovery of superconductivity in iron-based superconductor was $LaFeAsO_{1-x}F_x$ with the critical temperature 26 K in 2008 [1], Which has attracted increasing attention by the scientific community. The optimized critical temperature of the electron doped of $LaO_{1-x}F_xFeAs$ recorded by maximizing the external pressure which is 43 K and determined by high pressure of electrical resistance measurements [2]. For high temperature iron based two band superconductors, the last high critical temperature upraised to 57 K particularly double doped for $Sm_{0.95}La_{0.05}O_{0.85}F_{0.15}FeAs$ [3]. The most superconductors of 122 parent compounds are more interested with the investigation of physical properties because of single crystals growth, electronic and magnetic properties. Among ion based superconductor, 122 systems are the most popular and promising material for an application owing to the upper critical magnetic field and low anisotropy, specifically in hole doped $(Ba_{0.6}K_{0.4})Fe_2As_2$ with 38 K critical temperature have made excessive straggle [4].

The other 122 iron based system have provided a great interest which are recently systematic measurements of thermal conductivity and magnetic properties which have shown that $Ba(Fe_{1-x}Ni_x)_2As_2$ in the strongly over-doped regime exhibits unconventional superconductivity [5, 6]. Recently, two band model of nickel substitution for iron $BaFe_2As_2$ at 20 K transition temperature induce superconductivity by changing its magnetic order. This iron based superconductor specifically is appropriate for dealing with the wide-ranging process of the electronic properties. This electronic structure or properties performed by dopants to the system and changes its structure due to ionic difference.

Electron pairing is mediated by an electron-phonon interaction for conventional superconductors, and can be well understood within the microscopic-model developed

*Corresponding author: Tel: +251955215515
e-mail: teklelisanu21@gmail.com

by Bardeen-Copper-Schrieffer (BCS) superconductivity theory, developed in 1957 [7]. To explain the superconductivity in iron-based superconductor, electron-phonon coupling mechanism is not sufficient. This leads to another pairing mechanism which is spin fluctuation or magnetic interaction.

The superconducting performance is estimated from the critical temperature, critical current density, upper critical magnetic field and anisotropy. Even though iron-based superconductor has high upper-critical magnetic field but from its family, 111 compounds have small upper critical magnetic field compared to the other system or family [8-10]. The crucial advancement of upper-critical magnetic field for iron-based superconductor is next to the future of type-II superconductivity [11]. To investigate the upper-critical magnetic field for unconventional iron-based superconductors having enough concepts about its pairing formation for this special system is more significant even for further study.

With the application of external magnetic field in both planes, then the respected upper-critical magnetic field drops to zero and this is conscience of vanishing superconductivity. The most influential theory for dealing with the magnetic phase diagram of iron-based superconductor is Ginzburg-Landau theory [12]. The multiband iron-based superconductors of free energy density functional theory is described as the power series order parameters with district of transition temperature and using GL equations by minimization of free energy density function, these can designate the field delivery in superconductors.

In another way, the iron-based superconductor is quite promising for applications because its high upper critical magnetic field, and critical current density makes this system attractive for electrical power and magnetic application. So this formulation is the most fundamental technique that leads the experimentalists to check its feasibility using mathematical model.

2. Formulation of the Model

2.1. The of Upper-critical Magnetic Field

The phenomenological Ginzburg-Landau (GL) free energy density functional for two coupled superconducting order parameters Φ_1 and Φ_2 can be expressed as [14],

$$H_{sc} = H_1 + H_2 + H_{12} + \frac{H^2}{8\pi} \tag{1}$$

where

$$H_1 = \left(-\frac{\hbar^2}{2m_1}\right)\left|\left(\nabla - \frac{2ieA}{\hbar c}\right)\Phi_1\right|^2 - \alpha_1|\Phi_1|^2 + \frac{\beta_1}{2}|\Phi_1|^4 \tag{2}$$

$$H_2 = \left(-\frac{\hbar^2}{2m_2}\right)\left|\left(\nabla - \frac{2ieA}{\hbar c}\right)\Phi_2\right|^2 - \alpha_2|\Phi_2|^2 + \frac{\beta_2}{2}|\Phi_2|^4 \tag{3}$$

$$\begin{aligned} H_{12} = {} & \varepsilon(\Phi_1\Phi_2^* + \Phi_2\Phi_1^*) \\ & + \varepsilon_1\left(\left[\left(\nabla + \frac{2ieA}{\hbar c}\right)^*\Phi_1^*\left(\nabla - \frac{2ieA}{\hbar c}\right)\Phi_2\right]\right. \\ & \left. + \left[\left(\nabla + \frac{2ieA}{\hbar c}\right)^*\Phi_2^*\left(\nabla - \frac{2ieA}{\hbar c}\right)\Phi_1\right]\right) \end{aligned} \tag{4}$$

The terms H_1 and H_2 are conventional contributions from Φ_1 and Φ_2 and the term H_{12} describes the inter-band coupling of order parameters without the loss of generality'. $\frac{H^2}{8\pi}$ is the deposited energy in the local magnetic. The effective mass for each bands is denoted as m_1 and m_2 the coefficients ε and ε_1 describe the coupling of two order parameters (proximity effect) and their gradients (drag effect) respectively. α_i is the temperature-dependent parameter and β_i is temperature independent parameter [14]. $H = \nabla \times A$ is expected external magnetic field as a function of vector potential. So, by inserting eqs. (2-4) into eq. (1), we obtained,

$$\begin{aligned} H_{sc} = {} & -\frac{\hbar^2}{2m_1}\left|\left(\nabla - \frac{2ieA}{\hbar c}\right)\Phi_1\right|^2 - \alpha_1|\Phi_1|^2 + \frac{\beta_1}{2}|\Phi_1|^4 \\ & -\frac{\hbar^2}{2m_2}\left|\left(\nabla - \frac{2ieA}{\hbar c}\right)\Phi_2\right|^2 - \alpha_2|\Phi_2|^2 + \frac{\beta_2}{2}|\Phi_2|^4 \\ & +\varepsilon(\Phi_1\Phi_2^* + \Phi_2\Phi_1^*) + \varepsilon_1\left(\left[\left(\nabla - \frac{2ieA}{\hbar c}\right)^*\Phi_1^*\left(\nabla - \frac{2ieA}{\hbar c}\right)\Phi_2\right]\right. \\ & \left. +\left[\left(\nabla - \frac{2ieA}{\hbar c}\right)^*\Phi_2^*\left(\nabla - \frac{2ieA}{\hbar c}\right)\Phi_1\right]\right) + \frac{H^2}{8\pi} \end{aligned} \tag{5}$$

In order to obtain Ginzburg-Landau equation for two band model superconductors, we have minimized eq. (5) with respect to variations in the complex conjugate of the order parameters as follow,

$$\frac{\partial H_{sc}}{\partial \Phi_1^*} = 0 \text{ and } \frac{\partial H_{sc}}{\partial \Phi_2^*} = 0 \tag{6}$$

At $T \to T_c$, the cubic order parameter approach to zero, therefore using this idea and eq. (6), the minimized GL free energy density function is written respectively as follow,

$$-\frac{\hbar^2}{2m_1}\left(\nabla - \frac{2ieA}{\hbar c}\right)^2\Phi_1 - \alpha_1\Phi_1 + \varepsilon\Phi_2 + \varepsilon_1\left(\nabla - \frac{2ieA}{\hbar c}\right)^2\Phi_2 = 0 \tag{7}$$

and

$$-\frac{\hbar^2}{2m_2}\left(\nabla - \frac{2ieA}{\hbar c}\right)^2\Phi_2 - \alpha_2\Phi_2 + \varepsilon\Phi_1 + \varepsilon_1\left(\nabla - \frac{2ieA}{\hbar c}\right)^2\Phi_1 = 0 \tag{8}$$

Using matrix product form and balanced for Eqs. (7) and (8), it can be described as follows,

$$\begin{pmatrix} H_{11} & H_{12} \\ H_{21} & H_{22} \end{pmatrix}\begin{pmatrix}\Phi_1\\ \Phi_2\end{pmatrix} = \begin{pmatrix} -\frac{\hbar^2}{2m_2}\left(\nabla-\frac{2ieA}{\hbar c}\right)^2-\alpha_1 & \varepsilon+\varepsilon_1\left(\nabla-\frac{2ieA}{\hbar c}\right)^2 \\ \varepsilon+\varepsilon_1\left(\nabla-\frac{2ieA}{\hbar c}\right)^2 & -\frac{\hbar^2}{2m_2}\left(\nabla-\frac{2ieA}{\hbar c}\right)^2-\alpha_2 \end{pmatrix}\begin{pmatrix}\Phi_1\\ \Phi_2\end{pmatrix}=0 \quad (9)$$

In order to linearize the GL equations better associate time independent Schrödinger equation to eq. (9) under a magnetic field of harmonic oscillation having free moving particle of mass m_1 and m_2 and charge e^* becomes,

$$H_{11}\Phi_1 = -\frac{\hbar^2}{2m_1}\left(\nabla-\frac{2ieA}{\hbar c}\right)^2\Phi_1=E_{11}\Phi_1 \text{ and}$$
$$H_{22}\Phi_2 = -\frac{\hbar^2}{2m_2}\left(\nabla-\frac{2ieA}{\hbar c}\right)^2\Phi_2=E_{22}\Phi_2$$

Therefore having the above relation eq. (9) will be

$$\begin{pmatrix} E_{11}-\alpha_1 & \varepsilon+\varepsilon_1\left(\nabla-\frac{2ieA}{\hbar c}\right)^2 \\ \varepsilon+\varepsilon_1\left(\nabla-\frac{2ieA}{\hbar c}\right)^2 & E_{22}-\alpha_2 \end{pmatrix}\begin{pmatrix}\Phi_1\\ \Phi_2\end{pmatrix}=0 \quad (10)$$

In order to calculate the upper critical magnetic field, first it is very important to consider the energy eigen-values of the quantum harmonic oscillator. Since the lowest part of the quantum field can be approximated as a harmonic oscillation, therefore the lowest energy level has an energy $E_{11}=\frac{1}{2}\hbar\omega_1$ and $E_{22}=\frac{1}{2}\hbar\omega_2$ in these level any one calculates the upper-critical magnetic field at the ground state. At this level the oscillator frequency is $\omega_i=\frac{2eH_{c2}}{m_i c}$ with the vector potential of $A=H_{c2}x$ in one dimensional x direction. Therefore eq. (10) can be written as,

$$\begin{pmatrix} \frac{\hbar eH_{c2}}{m_1 c}-\alpha_1 & \varepsilon-\varepsilon_1\frac{2eH_{c2}}{\hbar c} \\ \varepsilon-\varepsilon_1\frac{2eH_{c2}}{\hbar c} & \frac{\hbar eH_{c2}}{m_2 c}-\alpha_1 \end{pmatrix}\begin{pmatrix}\Phi_1\\ \Phi_2\end{pmatrix}=0 \quad (11)$$

By having determinant and $m_1=m_2=m$ for eq. (11), the upper-critical magnetic field can be obtained as

$$\begin{vmatrix} \frac{\hbar eH_{c2}}{mc}-\alpha_1 & \varepsilon-\varepsilon_1\frac{2eH_{c2}}{\hbar c} \\ \varepsilon-\varepsilon_1\frac{2eH_{c2}}{\hbar c} & \frac{\hbar eH_{c2}}{mc}-\alpha_2 \end{vmatrix}=0 \quad (12)$$

Eq. (12) can be written as,

$$\left[\left(\frac{e\hbar}{mc}\right)^2-\frac{4e^2\varepsilon_1^2}{\hbar^2c^2}\right]H_{c2}^2-\left[\frac{e\hbar}{mc}(\alpha_1+\alpha_2)-\frac{4e\varepsilon\varepsilon_1}{\hbar c}\right]H_{c2} + \alpha_1\alpha_2-\varepsilon^2=0 \quad (13)$$

So, the solution for this quadratic equation will be,

$$H_{c2}=\frac{\frac{e\hbar}{mc}(\alpha_1+\alpha_2)-\frac{4e\varepsilon\varepsilon_1}{\hbar c}\pm \sqrt{\frac{e^2\hbar^2}{m^2c^2}[\alpha_1^2+\alpha_2^2]-\frac{2e^2\hbar^2}{m^2c^2}\alpha_1\alpha_2-\frac{8e^2\varepsilon\varepsilon_1}{mc^2}[\alpha_1+\alpha_2]+\frac{16e^2\varepsilon_1^2}{\hbar^2c^2}\alpha_1\alpha_2+\frac{4e^2\hbar^2\varepsilon^2}{m^2c^2}}}{2\left[\left(\frac{e\hbar}{mc}\right)^2-\frac{4e^2\varepsilon_1^2}{\hbar^2c^2}\right]} \quad (14)$$

For simplification we used $\alpha_1=\frac{\hbar^2}{2m\xi_1^2}$, $\alpha_2=\frac{\hbar^2}{2m\xi_2^2}$, $\varepsilon=\frac{\hbar^2}{2m\xi_{12}^2}$ to make scaling, where ξ_1, ξ_2, and ξ_{12} are the effective corresponding coherence lengths for each bands, $\varepsilon_1=\frac{\kappa\hbar^2}{2m}$ and $\Phi_0=\frac{2\pi\hbar}{e}$ are excitation energy with the mixing gradient inter-band and quantum flux respectively, therefore by inserting those variables lastly we got,

$$H_{c2}=\frac{\Phi_0}{2\pi(1-\kappa^2)}\left(\frac{1}{2\xi_1^2}-\frac{1}{2\xi_2^2}+\frac{\kappa}{\xi_{12}^2}\right)\pm\frac{\Phi_0}{2\pi(1-\kappa^2)} \left[\left(\frac{1}{2\xi_1^2}+\frac{1}{2\xi_2^2}-\frac{\kappa}{\xi_{12}^2}\right)^2-(1-\kappa^2)\left(\frac{1}{\xi_1^2\xi_2^2}-\frac{1}{\xi_{12}^4}\right)\right]^{\frac{1}{2}} \quad (15)$$

In order to solve this equation considering some cases is very important

The first case is that for: - $\left(\frac{1}{2\xi_1^2}+\frac{1}{2\xi_2^2}-\frac{\kappa}{\xi_{12}^2}\right)^2<<(1-\kappa^2)\left(\frac{1}{\xi_1^2\xi_2^2}-\frac{1}{\xi_{12}^4}\right)$, for this part the square root is complex. Therefore since the magnetic field is real, this solution is invalid.

The second case is that for: - $\left(\frac{1}{2\xi_1^2}+\frac{1}{2\xi_2^2}-\frac{\kappa}{\xi_{12}^2}\right)^2>>(1-\kappa^2)\left(\frac{1}{\xi_1^2\xi_2^2}-\frac{1}{\xi_{12}^4}\right)$, for this part the solution is valid and by employing Taylor binomial series expansions, the upper-critical magnetic field for eq. (15) has negative and positive value respectively as follow,

$$H_{c2}^{-}=\frac{\Phi_0}{2\pi}\frac{1}{2}\frac{\left(\frac{1}{\xi_1^2\xi_2^2}-\frac{1}{\xi_{12}^4}\right)}{\left(\frac{1}{2\xi_1^2}+\frac{1}{2\xi_2^2}-\frac{\kappa}{\xi_{12}^2}\right)}-\frac{1}{8}\frac{\Phi_0}{2\pi}\left(\frac{(1-\kappa^2)\left(\frac{1}{\xi_1^2\xi_2^2}-\frac{1}{\xi_{12}^4}\right)^2}{\left(\frac{1}{2\xi_1^2}+\frac{1}{2\xi_2^2}-\frac{\kappa}{\xi_{12}^2}\right)^3}\right) \quad (16)$$

$$H_{c2}^{+}=\frac{\Phi_0}{2\pi(1-\kappa^2)}\left(\frac{1}{2\xi_1^2}+\frac{1}{2\xi_2^2}-\frac{\kappa}{\xi_{12}^2}\right)$$
$$-\frac{\Phi_0}{2\pi}\frac{1}{2}\frac{\left(\frac{1}{\xi_1^2\xi_2^2}-\frac{1}{\xi_{12}^4}\right)}{\left(\frac{1}{2\xi_1^2}+\frac{1}{2\xi_2^2}-\frac{\kappa}{\xi_{12}^2}\right)}+\frac{1}{8}\frac{\Phi_0}{2\pi}\left(\frac{(1-\kappa^2)\left(\frac{1}{\xi_1^2\xi_2^2}-\frac{1}{\xi_{12}^4}\right)^2}{\left(\frac{1}{2\xi_1^2}+\frac{1}{2\xi_2^2}-\frac{\kappa}{\xi_{12}^2}\right)^3}\right) \quad (17)$$

The two band superconductor of GL theory is reduced to effective single band superconductor due to the case of drag effect, and in this case $\alpha_2 = \varepsilon = \varepsilon_1 = 0$. Therefore eq. (17) only the reduced theory to effective single band model and the upper-critical magnetic field have a solution with a physical meaning as follows,

$$H_{c2}=\frac{\Phi_0}{2\pi\xi_{12}^2}\left(\frac{\xi_{12}^2}{\xi_1^2}+\frac{\xi_{12}^2}{\xi_2^2}-2\kappa\right)$$
$$\left[\frac{1}{1-\kappa^2}-\frac{\frac{\xi_{12}^2}{\xi_1^2\xi_2^2}-1}{\left(\frac{\xi_{12}^2}{\xi_1^2}+\frac{\xi_{12}^2}{\xi_2^2}-2\kappa\right)^2}+\frac{(1-\kappa^2)\left(\frac{\xi_{12}^4}{\xi_1^2\xi_2^2}-1\right)^2}{\left(\frac{\xi_{12}^2}{\xi_1^2}+\frac{\xi_{12}^2}{\xi_2^2}-2\kappa\right)^4}\right] \quad (18)$$

By inserting the coherence length on the upper-critical magnetic field with the effect of anisotropy mass tensor for eq. (18) will be,

$$H_{c2}=\frac{\Phi_0}{2\pi\xi_{12}^2\sqrt{\sin^2\theta+\gamma^2\cos^2\theta}}\left(\frac{\xi_{12}^2}{\xi_1^2}+\frac{\xi_{12}^2}{\xi_2^2}-2\kappa\right)$$
$$\left[\frac{1}{1-\kappa^2}-\frac{\frac{\xi_{12}^2}{\xi_1^2\xi_2^2}-1}{\left(\frac{\xi_{12}^2}{\xi_1^2}+\frac{\xi_{12}^2}{\xi_2^2}-2\kappa\right)^2}+\frac{(1-\kappa^2)\left(\frac{\xi_{12}^4}{\xi_1^2\xi_2^2}-1\right)^2}{\left(\frac{\xi_{12}^2}{\xi_1^2}+\frac{\xi_{12}^2}{\xi_2^2}-2\kappa\right)^4}\right] \quad (19)$$

In isotropic bulk two-band superconductor, the gradient part of two order parameters have great significance, therefore the GL characteristics length and the upper-critical magnetic field of the two-band superconductor have physical insight.

Therefore expressing the effective coherence length as follows.

$$\frac{1}{\xi_{eff}^2}=\frac{1}{\xi_{12}^2}\left(\frac{\xi_{12}^2}{\xi_1^2}+\frac{\xi_{12}^2}{\xi_2^2}-2\kappa\right)$$
$$\left[\frac{1}{1-\kappa^2}-\frac{\frac{\xi_{12}^2}{\xi_1^2\xi_2^2}-1}{\left(\frac{\xi_{12}^2}{\xi_1^2}+\frac{\xi_{12}^2}{\xi_2^2}-2\kappa\right)^2}+\frac{(1-\kappa^2)\left(\frac{\xi_{12}^4}{\xi_1^2\xi_2^2}-1\right)^2}{\left(\frac{\xi_{12}^2}{\xi_1^2}+\frac{\xi_{12}^2}{\xi_2^2}-2\kappa\right)^4}\right] \quad (20)$$

So, eq. (19) will be,

$$H_{c2}(T)=\frac{\Phi_0}{2\pi\xi_{eff}^2(T)\sqrt{\sin^2\theta+\gamma^{-2}\cos^2\theta}} \quad (21)$$

Using the upper-critical magnetic field of eq. (21), we can determine the angle dependence of upper-critical magnetic field for isotropic effective masses at angle θ which is between c-axis and applied magnetic field at low temperature,

$$H_{c2}(\theta)=\frac{\Phi_0}{2\pi\xi_{eff}^2(0)\sqrt{\sin^2\theta+\gamma^{-2}\cos^2\theta}} \quad (22)$$

Using eq. (21) the $Ba(Fe_{1-x}Ni_x)_2As_2$ at 0 K, 1.75 anisotropy parameter [15], $\xi_{ab}(0)$ = 2.3 nm and $\xi_c(0)$ = 2.01 nm coherence length [16] and using $\Phi_0 = 2.0678 \times 10^{-15}$ Tm^2 will be,

$$H_{c2}(\theta)=\frac{32}{\sqrt{\sin^2\theta+0.32\cos^2\theta}} \quad (23)$$

This indicated the upper-critical magnetic field near to the critical temperature is dependent of angle θ [17].

Therefore using eq. (21) the applied magnetic field parallel to the direction of c-axis, the temperature dependence upper-critical magnetic field becomes,

$$H_{c2}^{\parallel c}(T)=\frac{\Phi_0}{2\pi\xi_{ab}^2(0)}\left[1-\left(\frac{T}{T_c}\right)^2\right] \quad (24)$$

In the ab-plane the GL coherence length $\xi_{ab}(T) = \xi_{ab}(0)\left[1-\left(\frac{T}{T_c}\right)^2\right]^{-\frac{1}{2}} = \xi_{ab}(0) = 2.3$ nm, at 0 K.

So, the final temperature dependence upper-critical magnetic field of eq. (24) will be,

$$H_{c2}^{\parallel c}(T)=47\left[1-\left(\frac{T}{T_c}\right)^2\right] \quad (25)$$

Using the same procedure for eq. (21) the temperature dependence of upper critical magnetic field with applied magnetic field perpendicular to the c-axis can be expressed as,

$$H_{c2}^{\perp c}(T)=\frac{\Phi_0}{2\pi\xi_{ab}(0)\xi_c(0)}\left[1-\left(\frac{T}{T_c}\right)^2\right] \quad (26)$$

So, having $\xi_{ab}(0)$ = 2.7 nm, $\xi_{ab}(0)$ = 2.7 nm and $\Phi_0 = 2.0678 \times 10^{-15}$ Tm^2 for eq. (26) becomes,

$$H_{c2}^{\perp c}(T)=82\left[1-\left(\frac{T}{T_c}\right)^2\right] \quad (27)$$

2.2. GL of coherence length and penetration depth

In order to characterize the phenomenological properties of a superconductor using GL model, the coherence has

to be considered. This characteristic length can be defined as,

$$\xi_{GL}(T) = \left(\frac{\hbar^2}{2m^*|\alpha(T)|}\right)^{\frac{1}{2}} \tag{28}$$

The coherence length can indicate the standard width of the transition layer of the order parameter Φ neighborhood of the boundary between a normal region and a superconducting region.

$\alpha(T)$ at the temperature less than the critical temperature can be described as $\alpha_i(T) = \alpha_0\left[1-\left(\frac{T}{T_c}\right)^2\right]$. Therefore the GL characteristics length with zero temperature $\xi_{GL}(0)$ is expressed as,

$$\xi_{GL}(T) = \xi_{GL}(0)\left[1-\left(\frac{T}{T_c}\right)^2\right]^{-\frac{1}{2}} \tag{29}$$

Therefore, by taking $\xi^{ab}_{GL}(0)$ and $\xi^{c}_{GL}(0)$ into consideration the final expression for each coherence length becomes respectively.

$$\xi^{ab}_{GL}(T) = 2.3\text{ nm}\left[1-\left(\frac{T}{T_c}\right)^2\right]^{-\frac{1}{2}} \tag{30}$$

$$\xi^{c}_{GL}(T) = 0.8\text{ nm}\left[1-\left(\frac{T}{T_c}\right)^2\right]^{-\frac{1}{2}} \tag{31}$$

The other very important phenomenological properties of a superconductor using GL model is the GL penetration depth (λ_{GL}) which penetrates a superconductor and surface current flows with a very thin thickness. this can be described as a function of superconducting electron density as follow,

$$\lambda_{GL}(T) = \left(\frac{mc^2}{16\pi e^2 n_s}\right)^{\frac{1}{2}} \tag{32}$$

When the superconducting electron density approaches to the total electron density at 0 K,

$$\lambda_{GL}(0) = \left(\frac{mc^2}{16\pi e^2 n_s}\right)^{\frac{1}{2}} \tag{33}$$

Using the two-fluid model or theory [18], the above equation will be,

$$\frac{n_s}{n} = \left[1-\left(\frac{T}{T_c}\right)^4\right] \tag{34}$$

Performing eq. (34) and (33) in eq. (32), we obtain,

$$\lambda_{GL}(T) = \lambda_{GL}(0)\left[1-\left(\frac{T}{T_c}\right)^4\right]^{-\frac{1}{2}} \tag{35}$$

Therefore, by having the experimental values of $\lambda^{ab}_{GL}(0)$ and $\lambda^{c}_{GL}(0)$, we have

$$\lambda^{ab}_{GL}(T) = 101\text{ nm}\left[1-\left(\frac{T}{T_c}\right)^4\right]^{-\frac{1}{2}} \tag{36}$$

$$\lambda^{c}_{GL}(T) = 248.6\text{ nm}\left[1-\left(\frac{T}{T_c}\right)^4\right]^{-\frac{1}{2}} \tag{37}$$

Using the experimental values for $Ba(Fe_{1-x}Ni_x)_2As_2$, the GL characteristic parameter κ becomes,

$$\kappa_c = \frac{\lambda^{ab}_{GL}(0)}{\xi^{ab}_{GL}(0)} = \frac{101\text{ nm}}{2.3\text{ nm}} = 43.9 \text{ and}$$

$$\kappa_{ab} = \frac{\lambda^{c}_{GL}(0)}{\xi^{ab}_{GL}(0)} = \frac{248.6\text{ nm}}{2.3\text{ nm}} = 108.1 \tag{38}$$

$$k = \frac{\kappa_{ab}}{\kappa_c} = 2.46 > \frac{1}{\sqrt{2}} \tag{39}$$

The GL characteristic parameter κ, shows the exact break point between type-I and type-II superconductors, which $\kappa = \frac{1}{\sqrt{2}}$, $\kappa < \frac{1}{\sqrt{2}}$ and $\kappa > \frac{1}{\sqrt{2}}$ apply for, type-I and type-II respectively. This idea was approved or experimented by Abrikosov [19]. Based on this the considerable system of this study for eq. (38), and we conclude that the iron based superconductor $Ba(Fe_{1-x}Ni_x)_2As_2$ is an example of type-II superconductors.

3. Results and Discussion

In this paper the angle and temperature dependence upper-critical magnetic field for field parallel and perpendicular to the symmetry axis, the GL characteristics lengths

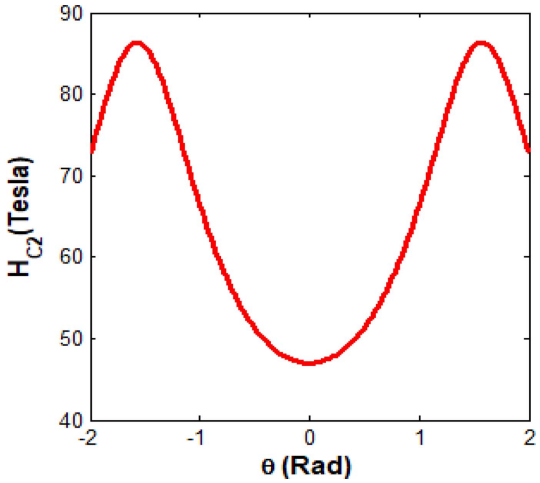

Fig. 1. (Color online) Dependency of upper critical magnetic field $H_{c2}(\theta)$ with the angle θ in $Ba(Fe_{1-x}Ni_x)_2As_2$.

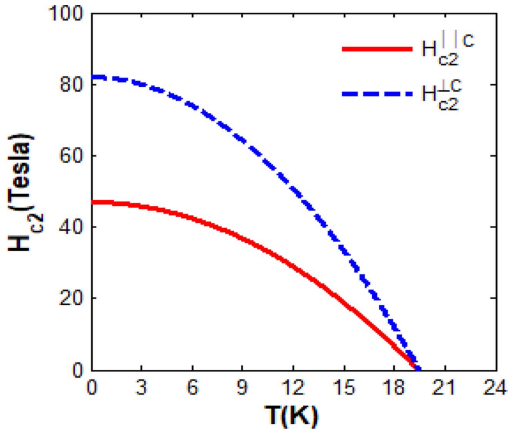

Fig. 2. (Color online) Temperature dependence of the upper critical magnetic field parallel and perpendicular to the symmetry axis in $Ba(Fe_{1-x}Ni_x)_2As_2$.

for parallel and perpendicular to the symmetry axis have been investigated using GL two band phenomenological model in $Ba(Fe_{1-x}Ni_x)_2As_2$ iron-based superconductor.

The angle dependence of upper-critical magnetic field in eq. (23) is the primarily mathematical expression, and its phase diagram has been shown in Fig. 1. From this figure the upper critical magnetic field increases from zero to ninety degree without linearly for $Ba(Fe_{1-x}Ni_x)_2As_2$ iron based system.

Next to this, the experimental values in eq. (25) and (27), the phase diagram of $H_{c2}^{\|c}$ and $H_{c2}^{\perp c}$ with temperature have been shown in Fig. 2. From this phase diagram both temperature dependent upper-critical magnetic fields decrease for increasing temperature in this considerable iron-based system. Similarly, using the experimental values for eqs. (30) and (31), the phase diagram of both GL

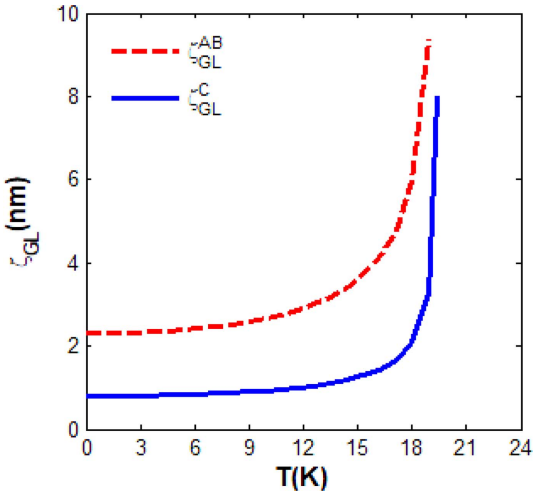

Fig. 3. (Color online) Ginzburg-Landau coherence length $\xi_{GL}(T)$ versus temperature in $Ba(Fe_{1-x}Ni_x)_2As_2$.

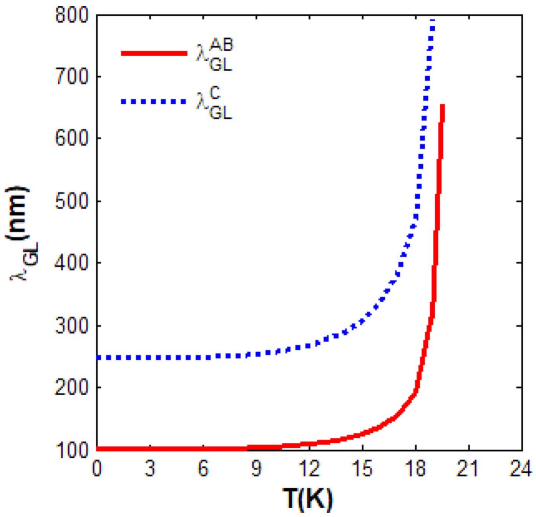

Fig. 4. (Color online) Ginzburg-Landau penetration depth $\xi_{GL}(T)$ versus temperature in $Ba(Fe_{1-x}Ni_x)_2As_2$.

coherence length with temperature have been shown in Fig. 3. So, this plot tells us both temperature dependence coherence lengths increase to the temperature and diverge to infinity at the critical temperature in this superconducting iron-based compound. Finally, by considering the experimental values in eqs. (36) and (37), the phase diagram of ξ_{GL}^{ab} and ξ_{GL}^{c} with temperature have been plotted in Fig. 4. In this phase diagram both GL penetration depth increased to the temperature and are diverged to infinity at the critical temperature in the superconductor $Ba(Fe_{1-x}Ni_x)_2As_2$.

4. Conclusion

In order to determine the phenomenological characteristics properties for two band iron-based superconductor, we used two-band Ginzburg-Landau (GL) model. Using this model the upper critical magnetic field, GL coherence length and GL penetration depth have been determined for $Ba(Fe_{1-x}Ni_x)_2As_2$ iron based superconductor and we have plotted the phase diagrams with temperature for each parameters. From these the GL coherence length and penetration depth are forcefully temperature dependent: this is the consequences of anisotropy nature and temperature dependence of upper-critical magnetic field in $Ba(Fe_{1-x}Ni_x)_2As_2$ two band model of iron based superconductor. This shows that the critical field along ab-plane ($H_{c2}^{\perp c}$) is quite different from critical field along c-axis ($H_{c2}^{\|c}$). As we have seen in Fig. 2 the two upper-critical magnetic fields decay to the temperature. The upper-critical magnetic field with angle theta is also shown in Fig. 1. Finally, the GL coherence length and

Ginzburg-Landau (GL) penetration depth with temperature have been plotted in Fig. 3 and Fig. 4, these indicate that both characteristic lengths diverge to infinity at the transition temperature. This theoretical investigation is consistent with the obtained experimental results [20].

References

[1] Y. Kamihara, T. Watanabe, M. Hirano, and H. Hosono, J. Am. Chem. Soc. **130**, 3296 (2008).
[2] H. Takahashi, K. Igawa, K. Arii, Y. Kamihara, M. Hirano, and H. Hosono, Nature **453**, 376 (2008).
[3] Nuwal, S. Kakani, and S. L. Kakani, SOP Transactions on Theoretical Physics **1**, 7 (2014).
[4] J. Yang, D. Hüvonen, U. Nagel, T. Rõõm, N. Ni, P. C. Canfield, S. L. Bud'ko, J. P. Carbotte, and T. Timusk, Phys. Rev. Lett. **102**, 187003 (2009).
[5] P. C. Canfield, S. L. Bud'ko, N. Ni, J. Q. Yan, and A. Kracher, Phys. Rev. B **80**, 060501 (2009).
[6] N. Ni, A. Thaler, J. Q. Yan, A. Kracher, E. Colombier, S. L. Bud'ko, P. C. Canfield, and S. T. Hannahs, Phys. Rev. B **82**, 024519 (2010).
[7] J. Bardeen, L. N. Cooper, and J. R. Schrieffer, Phys. Rev. **108**, 1175 (1957).
[8] I. R. Sheinand and A. I. Ivanovskii, Solid State Communications **150**, 152 (2010).
[9] Y. J. Song, J. S. Ghim, B. H. Min, Y. S. Kwon, M. H. Jung, and J.-S. Rhyee, Appl. Phys. Lett. **96**, 212508 (2010).
[10] X. Zhang and Y. Ma, Chinese Science Bulletin **58**, 986 (2013).
[11] E. Helfand and N. R. Werthamer, Phys. Rev. **147**, 288 (1966).
[12] N. R. Werthamer, E. Helfand, and P. C. Hohenberg, Phys. Rev. **147**, 295 (1966).
[13] J. Bardeen, L. N. Cooper, and J. R. Schrieffer, Phys. Rev. Lett. **108**, 1175 (1957).
[14] A. A. Golubov and A. E. Koshelev, Phys. Rev. B **68**, 104503 (2003).
[15] N. Werthamer, E. Helfand, and P. Hohenberg, Phys. Rev. **147**, 295 (1966).
[16] N. Barišić, D. Wu, M. Dressel, L. J. Li, G. H. Cao, and Z. A. Xu, Phys. Rev. B **82**, 054518 (2010).
[17] T. M. Mishonov, S. I. Klenov, and E. S. Penev, Phys. Rev. B **71**, 024520 (2005).
[18] C. J. Gorter and H. B. G. Casimir, Physica **1**, 306 (1934).
[19] A. A. Abrikosov, Soviet Physics JETP **5**, 1174 (1957).
[20] L. Fang, H. Luo, P. Cheng, Z. Wang, Y. Jia, G. Mu, B. Shen, I. I. Mazin, L. Shan, C. Ren, and H.-H. Wen, Phys. Rev. B **80**, 140508 (2009).